Connection between zero-energy Yu-Shiba-Rusinov states and 0-π transitions in magnetic Josephson junctions

Andreas Costa,* Jaroslav Fabian, and Denis Kochan
Institute for Theoretical Physics, University of Regensburg, 93040 Regensburg, Germany

(Received 6 March 2018; revised manuscript received 17 August 2018; published 24 October 2018)

We study theoretically the bound state spectrum and 0-π transitions in ballistic quasi-one-dimensional superconductor/ferromagnetic insulator/superconductor Josephson junctions. In addition to the Andreev bound states, stemming from the phase coherence, the magnetic barrier gives rise to qualitatively different Yu-Shiba-Rusinov (YSR) bound states with genuine spectral features and spin characteristics. We show that zero-energy YSR states are much more robust against the presence of scalar tunneling than their Andreev counterparts and also fingerprint a quantum phase transition from the junctions' 0 into the π phase, connected to a measurable reversal of the Josephson current; this evidence persists also in the presence of Rashba spin-orbit coupling.

DOI: 10.1103/PhysRevB.98.134511

I. INTRODUCTION

Since its discovery, superconductivity evolved into a most influential area in fundamental science and technology. While the exchange interaction in metals favors parallel spins [1], the s-wave pairing in superconductors promotes the formation of Cooper pairs with antiparallel spin alignments [2,3]. The competition of those two antagonistic interactions within one system leads to interesting physical phenomena [4–6]. Prominent examples are S/F/S Josephson junctions [7–15], in which a leakage of Cooper pairs from the superconducting (S) electrodes introduces a nontrivial pairing in the proximitized ferromagnet (F). In response to the spin-selective exchange splitting in the F, the induced order parameter oscillates with a characteristic spatial length [9,10]; depending on the thickness of the F, the phase difference between the two S electrodes can accumulate an intrinsic π shift. That is responsible for the reversal of the Josephson current direction in such a π state junction regime as compared to its (usual) 0 state counterpart.

Another realization of π Josephson junctions relies on the coupling of S electrodes via interacting quantum dots (QDs). Several theoretical works [16–27] showed that the junction regimes can be controlled by the strength of the lead-QD coupling and the QD charging energy. Experimental observations of 0-π transitions in S/F/S [28–31] and S/QD/S [6,32–48] Josephson junctions boosted hopes for their engineering and designed technological applications, counting qubits [49], quantum computing [50–52], and spintronics [4,53,54].

An unambiguous spectroscopic fingerprint of Josephson junctions is the formation of subgap Andreev bound states (ABSs) [55,56], which have been studied in single [44,45,47,48] and double [57] QD-coupled Josephson junctions. In the latter case, the ABSs hybridized to novel Andreev molecular states, which can eventually launch a platform for realizing Majorana physics [58–63]. However, understanding the spectral features of Josephson junctions in magnetic systems becomes more intricate since the magnetism breaks Cooper pairs and allows a creation of additional subgap bound states, commonly known as Yu-Shiba-Rusinov (YSR) states [64–67]. YSR states have been intensively studied in various systems, e.g., in S substrates hosting magnetic adatoms [68–75] or nanowires connecting normal/superconductor junctions [76,77].

In this paper, we investigate the subgap bound states in ballistic S/FI/S Josephson junctions with ultrathin barriers containing ferromagnetic insulators (FIs). The subgap states possess unique spectral [18,78] and *spin* characteristics that are tunable by tunneling strengths or the S phase difference. Moreover, magnetic tunneling causes an interesting interplay between ABSs and YSR states, modifying, for example, the quasiparticle density of states (DOS) [27,38]. We pay special attention to zero-energy YSR states which can signal topological superconductivity [79–81] and ground state phase transitions [82]. We clearly distinguish the 0 and π phases of the ballistic S/FI/S Josephson junctions [78,83,84] and unravel the 0-π transition mechanism on the microscopic level: the reversal of the tunneling of Cooper pairs in the YSR channel near zero energy stems from the ground state phase transition. Therefore, besides the two conventional mechanisms explaining 0-π transitions—(1) proximity-induced effects in S/F/S and (2) the interplay between the Fermi statistics and strong correlations in S/QD/S junctions—we concentrate on the third one: pair tunneling via the spectrally distinct YSR states at the interface of the magnetic FI barrier. To demonstrate the universality and the robustness of our mechanism, we also investigate 0-π transitions in S/FI/S Josephson junctions in the presence of Rashba spin-orbit coupling (SOC) [54,85] in the S leads, eventually showing the same qualitative behavior. Our findings offer a comprehensive understanding of 0-π transitions in Josephson junctions.

The paper is organized in the following way. In Sec. II, we introduce our theoretical model and study the bound state spectra for some important limiting cases. Section III briefly comments on the states' impact on the quasiparticle DOS.

*Corresponding author: andreas.costa@physik.uni-regensburg.de

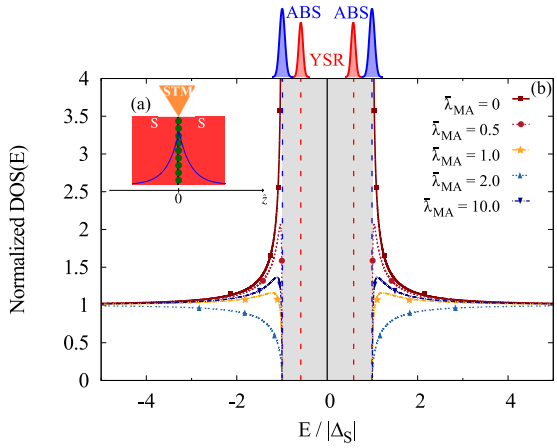

FIG. 1. (a) Josephson junction geometry; two superconductors (red) are separated by a thin ferromagnetic insulator (green dots). (b) Calculated quasiparticle DOS for $\bar{\lambda}_{SC} = 2$, zero phase difference, and various $\bar{\lambda}_{MA}$'s with pronounced coherence peak modulations. ABSs and YSR states inside the gap are schematically illustrated.

The main part of the paper is the analysis of the connection between the bound state spectrum and the Josephson current reversing 0-π transitions, which can be found in Secs. IV–VI.

II. THEORETICAL MODEL AND BOUND STATE SPECTRUM

We consider a vertical ballistic S/FI/S Josephson junction, consisting of two semi-infinite S regions that are separated by a thin deltalike tunnel barrier, simulating scalar and magnetic tunneling; see Fig. 1(a).

To analyze its spectral properties, we model the junction in terms of the stationary Bogoljubov–de Gennes (BdG) Hamiltonian [86],

$$\hat{H}_{\mathrm{BdG}} = \begin{bmatrix} \hat{H}_{\mathrm{e}} & \hat{\Delta}_{\mathrm{S}}(z) \\ \hat{\Delta}_{\mathrm{S}}^{\dagger}(z) & \hat{H}_{\mathrm{h}} \end{bmatrix}. \tag{1}$$

Here, $\hat{H}_{\mathrm{e}}=(-\hbar^2/2m\nabla^2 - \mu)\hat{\sigma}_0 + (\lambda_{\mathrm{SC}}\hat{\sigma}_0 + \lambda_{\mathrm{MA}}\hat{\sigma}_z)\delta(z)+ \hat{H}_{\mathrm{R}}$ represents the single-electron Hamiltonian and $\hat{H}_{\mathrm{h}} = -\hat{\sigma}_y\hat{H}_{\mathrm{e}}^{*}\hat{\sigma}_y$ its hole counterpart. Scalar and magnetic tunneling at the interface are modeled by deltalike potentials [87–89] with effective coupling strengths λ_{SC} and λ_{MA}, respectively, while $\hat{H}_{\mathrm{R}} = -\lambda_{\mathrm{R}}k_z\hat{\sigma}_y\Theta(z)$ accounts for Rashba SOC in the right lead, realized by a semiconducting electrode with proximity-induced superconductivity [90]. Spin matrices $\hat{\sigma}_0$ and $\hat{\sigma}_i$ stand for the two-by-two identity and the ith Pauli matrix. For the sake of simplicity, we assume a symmetric S/FI/S junction with equal quasiparticle masses m, the same chemical potential μ, and the transverse $\hat{z}$-dependent S order parameter $\hat{\Delta}_{\mathrm{S}}(z) = |\Delta_{\mathrm{S}}|\hat{\sigma}_0[\Theta(-z) + e^{i\phi_{\mathrm{S}}}\Theta(z)]$, where ϕ_{S} is the phase difference.

The general procedure for finding the eigencharacteristics of the Hamiltonian $\hat{H}_{\mathrm{BdG}}$, given by Eq. (1), is outlined in the Supplemental Material (SM) [91]. In what follows, we focus on quasi-one-dimensional (quasi-1D) junctions for which the thickness in the transverse $\hat{x}$ and $\hat{y}$ directions is much shorter than in the longitudinal $\hat{z}$ direction (higher-dimensional junctions bring no new features; see SM [91]). The particle-hole symmetric subgap eigenspectrum $E_n^{\pm}$ $(n = 1, 2)$ in the absence of SOC reads

$$\frac{E_n^{\pm}}{|\Delta_{\mathrm{S}}|} = \pm\sqrt{\frac{\left(\bar{\lambda}_{\mathrm{SC}}^2 - \bar{\lambda}_{\mathrm{MA}}^2\right)^2 + 8\left[2\cos^2\frac{\phi_{\mathrm{S}}}{2} + \frac{\bar{\lambda}_{\mathrm{SC}}^2}{2}\left(\cos^2\frac{\phi_{\mathrm{S}}}{2} + 1\right) + \frac{\bar{\lambda}_{\mathrm{MA}}^2}{2}\sin^2\frac{\phi_{\mathrm{S}}}{2} + (-1)^n|\bar{\lambda}_{\mathrm{MA}}|\sqrt{\sin^2\phi_{\mathrm{S}} + \bar{\lambda}_{\mathrm{SC}}^2\sin^2\frac{\phi_{\mathrm{S}}}{2} + \bar{\lambda}_{\mathrm{MA}}^2\cos^2\frac{\phi_{\mathrm{S}}}{2}}\right]}{\left(\bar{\lambda}_{\mathrm{SC}}^2 - \bar{\lambda}_{\mathrm{MA}}^2 + 4\right)^2 + 16\bar{\lambda}_{\mathrm{MA}}^2}}, \tag{2}$$

where $\bar{\lambda}_{\mathrm{SC}} = 2m\lambda_{\mathrm{SC}}/(\hbar^2 q_{\mathrm{F}})$ and $\bar{\lambda}_{\mathrm{MA}} = 2m\lambda_{\mathrm{MA}}/(\hbar^2 q_{\mathrm{F}})$ represent effective tunneling strengths with respect to the Fermi level (chemical potential μ); $q_{\mathrm{F}} = \sqrt{2m\mu}/\hbar$ stands for the corresponding Fermi momentum.

Let us briefly examine the main spectral characteristics of such Josephson junctions. Taking $\bar{\lambda}_{\mathrm{MA}} \to 0$, we recover the Andreev limit [11,92],

$$E_1^{\pm} = E_2^{\pm} = \pm|\Delta_{\mathrm{S}}|\sqrt{\frac{\bar{\lambda}_{\mathrm{SC}}^2 + 4\cos^2(\phi_{\mathrm{S}}/2)}{\bar{\lambda}_{\mathrm{SC}}^2 + 4}}. \tag{3}$$

Letting $\bar{\lambda}_{\mathrm{SC}} \to 0$ and $\phi_{\mathrm{S}} \to 0$, the spectrum complementary yields the celebrated YSR states [64,65,67],

$$E_1^{\pm} = \pm|\Delta_{\mathrm{S}}|\frac{\bar{\lambda}_{\mathrm{MA}}^2 - 4}{\bar{\lambda}_{\mathrm{MA}}^2 + 4}, \tag{4}$$

and two remaining states at $E_2^{\pm} = \pm|\Delta_{\mathrm{S}}|$, which coincide with the ABS at $\phi_{\mathrm{S}} = 0$; see Eq. (3). For that reason, we will refer to $E_1^{\pm}$ as the *YSR* and to $E_2^{\pm}$ as the *Andreev* branch.

Figure 2 shows a generic spin-resolved spectrum as a function of ϕ_{S} for various $\bar{\lambda}_{\mathrm{MA}}$. Generally, the Andreev branch is always closer to the gap edges than the YSR branch, serving as a spectroscopic fingerprint for distinguishing those states. While the Andreev states, given by Eq. (3), cross zero energy only for a transparent interface and phase differences $\phi_{\mathrm{S}} = \pi \pmod{2\pi}$ [92], Eq. (2) suggests that additional magnetic tunneling supports zero-energy YSR states in a wide range of

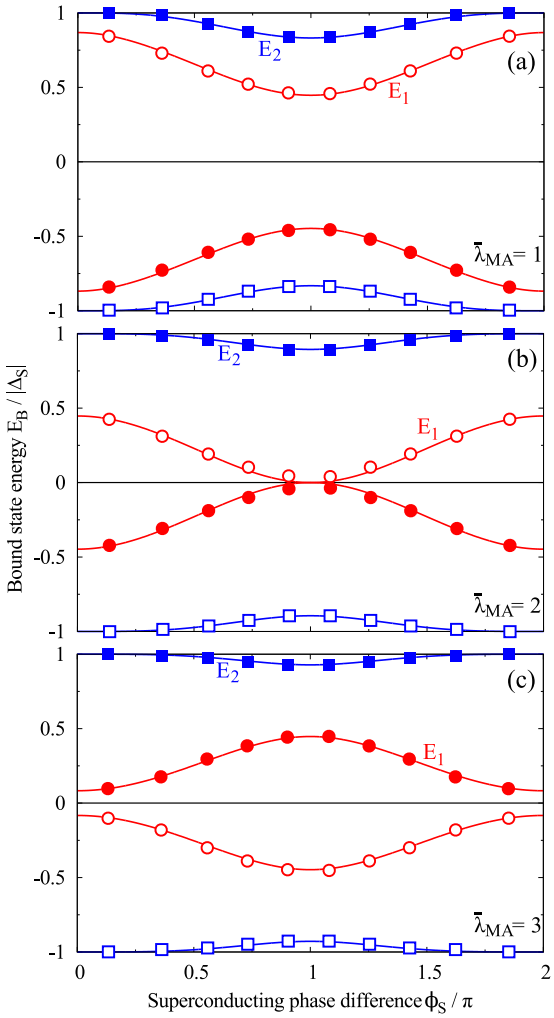

FIG. 2. Spin-resolved bound state energies E_1 and E_2 of the YSR (red) and the Andreev (blue) states as functions of ϕ_S for $\bar{\lambda}_{SC} = 2$ and various $\bar{\lambda}_{MA}$'s given in the plots; Rashba SOC is absent. Filled (empty) circles indicate spin up (down) YSR and filled (empty) squares spin up (down) Andreev states.

parameters. Analyzing Eq. (2), one sees that for $0 \leqslant \bar{\lambda}_{MA}^2 - \bar{\lambda}_{SC}^2 \leqslant 4$, there always exists a ϕ_S for which the YSR branch crosses zero energy; see Fig. 2. The corresponding ϕ_S comes as a solution of

$$\bar{\lambda}_{MA} = \pm\sqrt{\bar{\lambda}_{SC}^2 + 4\cos^2(\phi_S/2)}\,. \tag{5}$$

III. MODULATION OF QUASIPARTICLE DOS

The subgap states strongly impact the quasiparticle DOS. Figure 1(b) shows the DOS for $\bar{\lambda}_{SC} = 2$ and different $\bar{\lambda}_{MA}$'s at zero phase difference (for methodology, see SM [91]). Without magnetic tunneling, the spectrum only consists of ABS and the quasiparticle spectrum shows the standard BCS-like DOS. Gradually growing $\bar{\lambda}_{MA}$, the spectrum also contains YSR states that move to the gap center. As a consequence, a part of spectral weight is taken into the gap and the quasiparticle coherence peaks modify. A similar peak structure was identified in quantum-dot experiments [43,47]. Raising $\bar{\lambda}_{MA}$, the quasiparticle spectral peaks become unprecedentedly suppressed and disappear when the YSR states cross zero energy. A further increase of $\bar{\lambda}_{MA}$ shifts the bound states back towards the gap edges and, simultaneously, the quasiparticle DOS rises again.

IV. QUALITATIVE ANALYSIS—GROUND STATE PHASE TRANSITION

We see from Fig. 2 that the ABSs do not change spins with evolving ϕ_S, whereas the YSR states effectively "flip" spins when crossing zero energy. The states' spin ordering reflects important ground state properties, which we briefly discuss. Without the deltalike terms in $\hat{H}_e$ and $\hat{H}_h$, absent SOC, and for $\phi_S = 0$, the BdG Hamiltonian $\hat{H}_{BdG}$, given by Eq. (1), can be easily diagonalized. Denoting by $\alpha^\dagger$ (α) the creation (annihilation) operators for the BdG eigenmodes with positive energies and by $\beta^\dagger$ (β) the corresponding operators for negative energies, the BCS ground state $|\Omega\rangle$ is a Slater product over the occupied and unoccupied eigenmodes,

$$|\Omega\rangle = \prod_{\mathbf{k}} \alpha_{\mathbf{k},\uparrow}\alpha_{-\mathbf{k},\downarrow}\beta^\dagger_{\mathbf{k},\uparrow}\beta^\dagger_{-\mathbf{k},\downarrow}|0\rangle, \tag{6}$$

where $|0\rangle$ represents the Fermi vacuum.

What happens to $|\Omega\rangle$ when adding a deltalike exchange interaction, parameterized by λ_{MA}? For simplicity, let us start with zero λ_{SC} and ϕ_S. Assuming a small positive λ_{MA}, spin up states have higher energy than their spin down counterparts. This means that initially degenerate quasiparticle eigenmodes spin split and form spatially (quasi)localized impurity subgap states. Anticipating the results of Eq. (2) for $\lambda_{SC} = 0$ and $\phi_S = 0$, we denote the localized states with positive energies $0 < E_1^+ < E_2^+ \simeq |\Delta_S|$ as $|\psi_{YSR,\downarrow}\rangle$ and $|\psi_{A,\uparrow}\rangle$, and states with negative energies $-|\Delta_S| \simeq E_2^- < E_1^- < 0$ as $|\psi_{A,\downarrow}\rangle$ and $|\psi_{YSR,\uparrow}\rangle$; see Fig. 3. Generally, the states $|\psi_{YSR,\uparrow}\rangle$ and $|\psi_{YSR,\downarrow}\rangle$ are shifted more towards the center of the gap than $|\psi_{A,\downarrow}\rangle$ and $|\psi_{A,\uparrow}\rangle$ for $\lambda_{MA} > 0$, and hence become spatially more localized around the impurity. With a further increase of λ_{MA}, the energy of $|\psi_{YSR,\downarrow}\rangle$ continuously lowers, while that of $|\psi_{YSR,\uparrow}\rangle$ rises. Before reaching the critical value $\lambda_{MA}^{crit.} \sim \xi_{BCS}|\Delta_S|$ (ξ_{BCS} is the BCS coherence length), $|\psi_{YSR,\downarrow}\rangle$ remains unoccupied and $|\psi_{YSR,\uparrow}\rangle$ occupied; see Fig. 3(a). Denoting the corresponding creation (annihilation) operators for $|\psi_{A,\sigma}\rangle$ and $|\psi_{YSR,\sigma}\rangle$ by $A_\sigma^\dagger$ (A_σ) and $Y_\sigma^\dagger$ (Y_σ), respectively, we expect the ground state below $\lambda_{MA}^{crit.}$ to be in the form

$$|\Omega_<\rangle \sim A_\uparrow Y_\downarrow Y_\uparrow^\dagger A_\downarrow^\dagger \prod_{\mathbf{n}} \tilde{\alpha}_{\mathbf{n},\uparrow}\tilde{\alpha}_{-\mathbf{n},\downarrow}\tilde{\beta}^\dagger_{\mathbf{n},\uparrow}\tilde{\beta}^\dagger_{-\mathbf{n},\downarrow}|0\rangle. \tag{7}$$

The tilde operators have the same meaning as before—quasiparticle eigenmodes (now perturbed) with energies above and below the gap [93]. Increasing λ_{MA} over the critical $\lambda_{MA}^{crit.}$, the energy of $|\psi_{YSR,\downarrow}\rangle$ becomes smaller than that of $|\psi_{YSR,\uparrow}\rangle$ and, therefore, the relative occupations of both states interchange; see Fig. 3(b). The ground state wave function above $\lambda_{MA}^{crit.}$ is now expected to be

$$|\Omega_>\rangle \sim A_\uparrow Y_\uparrow Y_\downarrow^\dagger A_\downarrow^\dagger \prod_{\mathbf{n}} \tilde{\alpha}_{\mathbf{n},\uparrow}\tilde{\alpha}_{-\mathbf{n},\downarrow}\tilde{\beta}^\dagger_{\mathbf{n},\uparrow}\tilde{\beta}^\dagger_{-\mathbf{n},\downarrow}|0\rangle\,. \tag{8}$$

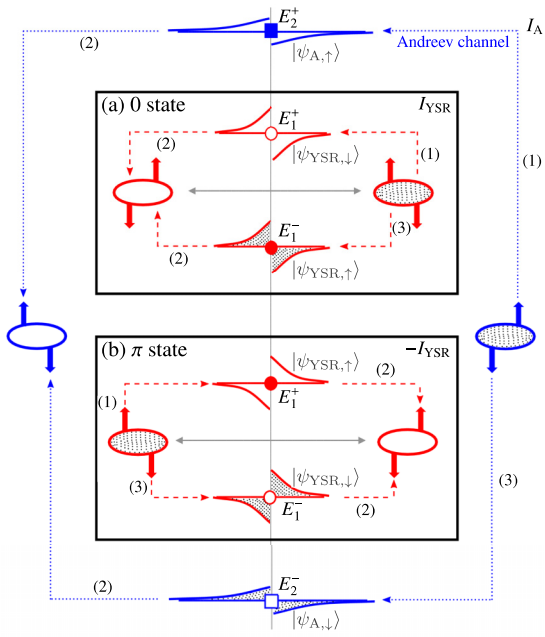

FIG. 3. Schematic picture of 0 and π ground states, and the associated transfer of Cooper pairs. Full (empty) squares/circles display spin up (down) Andreev/YSR states; the states at energies $E_2^{\pm}$ and $E_1^{\pm}$ are labeled as $|\psi_{\mathrm{A},\sigma}\rangle$ and $|\psi_{\mathrm{YSR},\sigma}\rangle$. The sketched evanescent tails indicate the spatial electron-hole density difference for a given $|\psi\rangle$. Occupied states and Cooper pairs are shaded. The dotted (blue) lines describe the Cooper pair transfer via the Andreev channel (current I_{A}) and the dashed (red) lines via the YSR channel (current I_{YSR}). The individual steps (1)–(3) are described in the text. The 0 state junction is displayed in (a) and the π state junction in (b). The change of the YSR spectral properties at the 0-π transition reverses I_{YSR}, while I_{A} remains unchanged.

The former ground state $|\Omega_<\rangle$ has a modified spin content inside the gap when compared to $|\Omega_>\rangle$, so both are in distinct quantum states, which we correspondingly call the 0 and π phases. Turning on λ_{SC} and ϕ_{S}, the bound state energies evolve in a complex way—see Eq. (2) for $\lambda_{\mathrm{SC}} \neq 0$ and $\phi_{\mathrm{S}} \neq 0$—nevertheless, crossings at zero energy again indicate changes in the spin ordering of the ground states. Thus, reversals of the Josephson current at 0-π transitions in ballistic S/FI/S Josephson junctions are interpreted in terms of a *change of the ground state spin order*.

V. 0-π TRANSITIONS IN JOSEPHSON CURRENT

Knowing the phase dependence of the bound state spectrum, we can obtain the Josephson current [94] $I_{\mathrm{J}}(\phi_{\mathrm{S}}) = -\frac{e}{\hbar}\sum_{n=1}^{2}[(\frac{\partial E_n^+}{\partial \phi_{\mathrm{S}}})\tanh(\frac{E_n^+}{2k_{\mathrm{B}}T})]$; e stands for the (positive) elementary charge and k_{B} is Boltzmann's constant. From the experimental point of view, it is common to measure the critical Josephson current $I^{\mathrm{crit.}} = \max_{\phi_{\mathrm{S}}}\{|I_{\mathrm{J}}(\phi_{\mathrm{S}})|\}$ and the corresponding critical S phase $\phi_{\mathrm{S}}^{\mathrm{crit.}}$. By tuning ϕ_{S} to its critical value and performing scanning tunneling spectroscopy/scanning tunneling microscopy (STS/STM) in the vicinity of the interface, one could explore the spectral properties of the subgap states. Figure 4(a) displays the dependence of $I^{\mathrm{crit.}}$ on the tunneling strengths. For each $\bar{\lambda}_{\mathrm{SC}}$, one finds

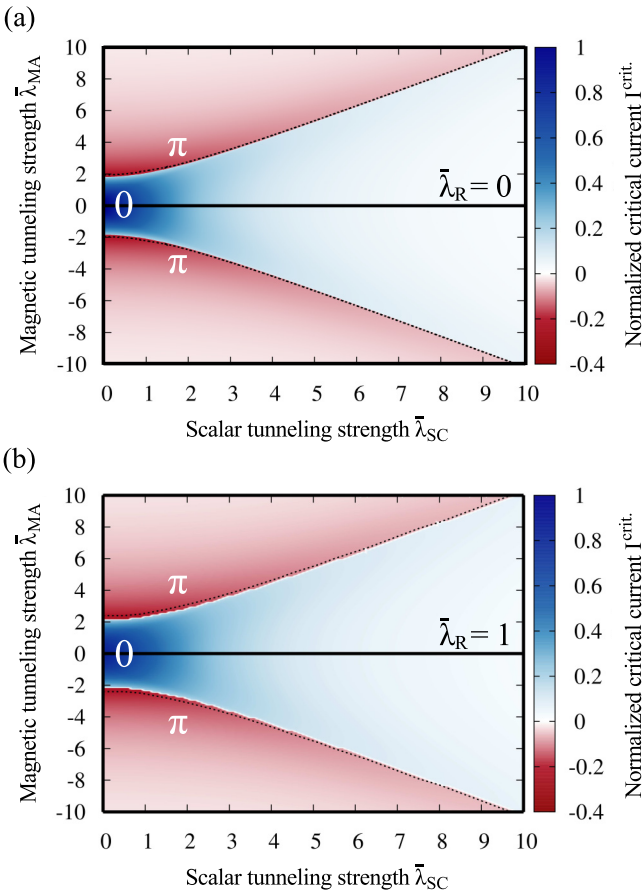

FIG. 4. (a) Contour plot of the normalized critical current $eI^{\mathrm{crit.}}R_{\mathrm{S}}/(\pi|\Delta_{\mathrm{S}}|)$ (R_{S} is Sharvin's resistance) as a function of $\bar{\lambda}_{\mathrm{SC}}$ and $\bar{\lambda}_{\mathrm{MA}}$ in the absence of Rashba SOC at zero temperature. Blue and red regions represent 0 and π regimes with positive and negative $I^{\mathrm{crit.}}$. The transition lines separating the two phases are displayed by white borderlines; the parameters at which zero-energy YSR states emerge are shown by dashed lines. (b) Same calculations in the additional presence of moderate Rashba SOC, $\bar{\lambda}_{\mathrm{R}} = m\lambda_{\mathrm{R}}/(\hbar^2 q_{\mathrm{F}}) = 1$.

a $\bar{\lambda}_{\mathrm{MA}}$ at which the Josephson current's direction reverses, indicating transitions from 0 to π regimes. The maximal current in the 0 state is twice as large as in the π state; moreover, as expected, the 0-π transition lines coincide with the contours signifying the formation of zero-energy YSR states. In Fig. 4(b), we show similar, fully numerical calculations in the presence of moderate Rashba SOC in the right electrode. Modulating the Rashba SOC by electrical gating [95,96] can efficiently tune 0-π transitions. Nevertheless, there is still a clear coincidence between the 0-π transition lines and the zero-energy YSR states, although SOC inevitably introduces an intrinsic shift to the current-phase relation. This causes slight deviations at weak tunnelings.

VI. ZERO-ENERGY YSR STATES AND REVERSAL OF JOSEPHSON CURRENT

To connect the zero-energy YSR states with the reversal of the Josephson current, one needs the bound state wave

functions. The full calculation is rather technical; see SM [91]. Here, we qualitatively illustrate the main mechanism. Figure 3 schematically shows the Andreev (blue dotted lines) and YSR (red dashed lines) channels, transporting Cooper pairs across the barrier. To understand the transport direction of one Cooper pair, we split each occupied and unoccupied bound state into its electronlike and holelike component and read out the corresponding electron-hole density difference. This is qualitatively illustrated by the sketched evanescent tails in Fig. 3 for the corresponding $|\psi_{\mathrm{A},\sigma}\rangle$ and $|\psi_{\mathrm{YSR},\sigma}\rangle$ states; upward (downward) tails indicate electron (hole) dominance. For the ABS, there is always an electronlike excess in the left and a holelike excess in the right S. This means that the electrons forming a Cooper pair are transferred via the Andreev channel from the right into the left superconductor by the individual steps (1)–(3). In (1), a spin up electron tunnels to an empty state at positive energy E_2^+. In (2), this electron pairs with a spin down electron residing in the occupied state at energy E_2^-, creating a spin-singlet Cooper pair in the left superconductor; finally, the remaining electron from the initial Cooper pair fills the vacant state at E_2^-. The situation for the YSR channel is different. In the 0 state, shown by Fig. 3(a), the YSR states also show electronlike excess on the left side and holelike excess on the right side of the barrier. Hence, the previous mechanism still holds and Cooper pairs are also transferred from right to left. In total, both current contributions add together, $I_{\mathrm{A}} + I_{\mathrm{YSR}}$. Contrarily, in the π phase, the spin-resolved electron and hole content of the YSR states spatially change and, therefore, the YSR states now drive Cooper pairs from left to right, i.e., against the direction of the Andreev channel. The total current is then $I_{\mathrm{A}} - I_{\mathrm{YSR}}$. Since the transition probabilities of the activation step (1) are proportional to $e^{-E_n^+/|\Delta_S|}$ and $E_1^+ < E_2^+$, the YSR contribution is generally dominant and, therefore, a reversal of I_{YSR} also reverses the total Josephson current. This qualitative explanation is fully consistent with our presented calculations.

VII. SUMMARY

We analyzed spectral and transport characteristics associated with Andreev and YSR states in magnetic Josephson junctions in terms of experimentally tunable parameters and showed that certain combinations of these parameters lead to zero-energy YSR states. Such states serve as a clear fingerprint of quantum phase transitions in the junctions' ground state. Particularly, we demonstrated that this phase transition coincides with the Josephson current reversing 0-π transitions. This coincidence between zero-energy YSR states and 0-π transitions persists also in the presence of Rashba SOC in one electrode.

ACKNOWLEDGMENTS

This work was supported by DFG SFB Grant No. 689 and DFG SFB Grant No. 1277 (B07). This project has received funding from the European Union's Horizon 2020 research and innovation programme under Grant Agreement No. 696656 and the International Doctorate Program Topological Insulators of the Elite Network of Bavaria.

[1] E. C. Stoner, Proc. R. Soc. London A: Math. Phys. Engineer. Sci. **169**, 339 (1939).
[2] J. Bardeen, L. N. Cooper, and J. R. Schrieffer, Phys. Rev. **106**, 162 (1957).
[3] J. Bardeen, L. N. Cooper, and J. R. Schrieffer, Phys. Rev. **108**, 1175 (1957).
[4] M. Eschrig, Phys. Today **64**, 43 (2011).
[5] J. Linder and J. W. A. Robinson, Nat. Phys. **11**, 307 (2015).
[6] E. C. Gingrich, B. M. Niedzielski, J. A. Glick, Y. Wang, D. L. Miller, R. Loloee, W. P. Pratt Jr, and N. O. Birge, Nat. Phys. **12**, 564 (2016).
[7] L. N. Bulaevskii, V. V. Kuzii, and A. A. Sobyanin, Pis'ma Zh. Eksp. Teor. Fiz. **25**, 314 (1977) [JETP Lett. **25**, 290 (1977)].
[8] A. I. Buzdin, L. N. Bulaevskii, and S. V. Panyukov, Pis'ma Zh. Eksp. Teor. Fiz. **35**, 147 (1982) [JETP Lett. **35**, 178 (1982)].
[9] A. V. Andreev, A. I. Buzdin, and R. M. Osgood, Phys. Rev. B **43**, 10124 (1991).
[10] E. A. Demler, G. B. Arnold, and M. R. Beasley, Phys. Rev. B **55**, 15174 (1997).
[11] A. A. Golubov, M. Y. Kupriyanov, and E. Il'ichev, Rev. Mod. Phys. **76**, 411 (2004).
[12] A. I. Buzdin, Rev. Mod. Phys. **77**, 935 (2005).
[13] F. S. Bergeret, A. F. Volkov, and K. B. Efetov, Rev. Mod. Phys. **77**, 1321 (2005).
[14] G. Annunziata, H. Enoksen, J. Linder, M. Cuoco, C. Noce, and A. Sudbø, Phys. Rev. B **83**, 144520 (2011).
[15] A. Costa, P. Högl, and J. Fabian, Phys. Rev. B **95**, 024514 (2017).
[16] L. I. Glazman and K. A. Matveev, Pis'ma Zh. Eksp. Teor. Fiz. **49**, 570 (1989) [JETP Lett. **49**, 659 (1989)].
[17] A. A. Clerk and V. Ambegaokar, Phys. Rev. B **61**, 9109 (2000).
[18] E. Vecino, A. Martín-Rodero, and A. Levy Yeyati, Phys. Rev. B **68**, 035105 (2003).
[19] M.-S. Choi, M. Lee, K. Kang, and W. Belzig, Phys. Rev. B **70**, 020502 (2004).
[20] F. Siano and R. Egger, Phys. Rev. Lett. **93**, 047002 (2004); **94**, 039902(E) (2005).
[21] J. Bauer, A. Oguri, and A. C. Hewson, J. Phys. Condens. Matter **19**, 486211 (2007).
[22] C. Karrasch, A. Oguri, and V. Meden, Phys. Rev. B **77**, 024517 (2008).
[23] T. Meng, S. Florens, and P. Simon, Phys. Rev. B **79**, 224521 (2009).
[24] D. J. Luitz and F. F. Assaad, Phys. Rev. B **81**, 024509 (2010).
[25] A. Martín-Rodero and A. L. Yeyati, Adv. Phys. **60**, 899 (2011).
[26] D. J. Luitz, F. F. Assaad, T. Novotný, C. Karrasch, and V. Meden, Phys. Rev. Lett. **108**, 227001 (2012).
[27] G. Kiršanskas, M. Goldstein, K. Flensberg, L. I. Glazman, and J. Paaske, Phys. Rev. B **92**, 235422 (2015).
[28] V. V. Ryazanov, V. A. Oboznov, A. Y. Rusanov, A. V. Veretennikov, A. A. Golubov, and J. Aarts, Phys. Rev. Lett. **86**, 2427 (2001).

[29] T. Kontos, M. Aprili, J. Lesueur, F. Genêt, B. Stephanidis, and R. Boursier, Phys. Rev. Lett. **89**, 137007 (2002).

[30] J. W. A. Robinson, S. Piano, G. Burnell, C. Bell, and M. G. Blamire, Phys. Rev. Lett. **97**, 177003 (2006).

[31] A. K. Feofanov, V. A. Oboznov, V. V. Bol'ginov, J. Lisenfeld, S. Poletto, V. V. Ryazanov, A. N. Rossolenko, M. Khabipov, D. Balashov, A. B. Zorin, P. N. Dmitriev, V. P. Koshelets, and A. V. Ustinov, Nat. Phys. **6**, 593 (2010).

[32] M. R. Buitelaar, T. Nussbaumer, and C. Schönenberger, Phys. Rev. Lett. **89**, 256801 (2002).

[33] H. I. Jørgensen, T. Novotný, K. Grove-Rasmussen, K. Flensberg, and P. E. Lindelof, Nano Lett. **7**, 2441 (2007).

[34] A. Eichler, R. Deblock, M. Weiss, C. Karrasch, V. Meden, C. Schönenberger, and H. Bouchiat, Phys. Rev. B **79**, 161407 (2009).

[35] R. S. Deacon, Y. Tanaka, A. Oiwa, R. Sakano, K. Yoshida, K. Shibata, K. Hirakawa, and S. Tarucha, Phys. Rev. Lett. **104**, 076805 (2010).

[36] J.-D. Pillet, C. H. L. Quay, P. Morfin, C. Bena, A. L. Yeyati, and P. Joyez, Nat. Phys. **6**, 965 (2010).

[37] K. J. Franke, G. Schulze, and J. I. Pascual, Science **332**, 940 (2011).

[38] E. J. H. Lee, X. Jiang, R. Aguado, G. Katsaros, C. M. Lieber, and S. De Franceschi, Phys. Rev. Lett. **109**, 186802 (2012).

[39] R. Maurand, T. Meng, E. Bonet, S. Florens, L. Marty, and W. Wernsdorfer, Phys. Rev. X **2**, 011009 (2012); **2**, 019901(E) (2012).

[40] W. Chang, V. E. Manucharyan, T. S. Jespersen, J. Nygård, and C. M. Marcus, Phys. Rev. Lett. **110**, 217005 (2013).

[41] B.-K. Kim, Y.-H. Ahn, J.-J. Kim, M.-S. Choi, M.-H. Bae, K. Kang, J. S. Lim, R. López, and N. Kim, Phys. Rev. Lett. **110**, 076803 (2013).

[42] J.-D. Pillet, P. Joyez, R. Žitko, and M. F. Goffman, Phys. Rev. B **88**, 045101 (2013).

[43] A. Kumar, M. Gaim, D. Steininger, A. Levy Yeyati, A. Martín-Rodero, A. K. Hüttel, and C. Strunk, Phys. Rev. B **89**, 075428 (2014).

[44] E. J. H. Lee, X. Jiang, M. Houzet, R. Aguado, C. M. Lieber, and S. De Franceschi, Nat. Nanotechnol. **9**, 79 (2014).

[45] R. Delagrange, D. J. Luitz, R. Weil, A. Kasumov, V. Meden, H. Bouchiat, and R. Deblock, Phys. Rev. B **91**, 241401 (2015).

[46] A. Assouline, C. Feuillet-Palma, A. Zimmers, H. Aubin, M. Aprili, and J.-C. Harmand, Phys. Rev. Lett. **119**, 097701 (2017).

[47] S. Li, N. Kang, P. Caroff, and H. Q. Xu, Phys. Rev. B **95**, 014515 (2017).

[48] D. J. van Woerkom, A. Proutski, B. van Heck, D. Bouman, J. I. Vayrynen, L. I. Glazman, P. Krogstrup, J. Nygard, L. P. Kouwenhoven, and A. Geresdi, Nat. Phys. **13**, 876 (2017).

[49] T. Yamashita, K. Tanikawa, S. Takahashi, and S. Maekawa, Phys. Rev. Lett. **95**, 097001 (2005).

[50] L. B. Ioffe, V. B. Geshkenbein, M. V. Feigel'man, A. L. Fauchère, and G. Blatter, Nature (London) **398**, 679 (1999).

[51] J. E. Mooij, T. P. Orlando, L. Levitov, L. Tian, C. H. van der Wal, and S. Lloyd, Science **285**, 1036 (1999).

[52] M. H. Devoret and R. J. Schoelkopf, Science **339**, 1169 (2013).

[53] I. Žutić, J. Fabian, and S. Das Sarma, Rev. Mod. Phys. **76**, 323 (2004).

[54] J. Fabian, A. Matos-Abiague, C. Ertler, P. Stano, and I. Žutić, Acta Phys. Slovaca **57**, 565 (2007).

[55] A. F. Andreev, Zh. Eksp. Teor. Fiz. **46**, 1823 (1964) [J. Exp. Theor. Phys. **19**, 1228 (1964)].

[56] A. F. Andreev, Zh. Eksp. Teor. Fiz. **49**, 655 (1966) [J. Exp. Theor. Phys. **22**, 455 (1966)].

[57] Z. Su, A. B. Tacla, M. Hocevar, D. Car, S. R. Plissard, E. P. A. M. Bakkers, A. J. Daley, D. Pekker, and S. M. Frolov, Nat. Commun. **8**, 585 (2017).

[58] L. Fu and C. L. Kane, Phys. Rev. Lett. **100**, 096407 (2008).

[59] Y. Oreg, G. Refael, and F. von Oppen, Phys. Rev. Lett. **105**, 177002 (2010).

[60] M. Duckheim and P. W. Brouwer, Phys. Rev. B **83**, 054513 (2011).

[61] V. Mourik, K. Zuo, S. M. Frolov, S. R. Plissard, E. P. A. M. Bakkers, and L. P. Kouwenhoven, Science **336**, 1003 (2012).

[62] L. P. Rokhinson, X. Liu, and J. K. Furdyna, Nat. Phys. **8**, 795 (2012).

[63] S. Nadj-Perge, I. K. Drozdov, J. Li, H. Chen, S. Jeon, J. Seo, A. H. MacDonald, B. A. Bernevig, and A. Yazdani, Science **346**, 602 (2014).

[64] L. Yu, Acta Phys. Sin. **21**, 75 (1965).

[65] H. Shiba, Progr. Theoret. Phys. **40**, 435 (1968).

[66] H. Shiba and T. Soda, Progr. Theoret. Phys. **41**, 25 (1969).

[67] A. I. Rusinov, Zh. Eksp. Teor. Fiz. **9**, 146 (1968) [JETP Lett. **9**, 85 (1969)].

[68] K. Satori, H. Shiba, O. Sakai, and Y. Shimizu, J. Phys. Soc. Jpn. **61**, 3239 (1992).

[69] J. Simonin and R. Allub, Phys. Rev. Lett. **74**, 466 (1995).

[70] M. I. Salkola, A. V. Balatsky, and J. R. Schrieffer, Phys. Rev. B **55**, 12648 (1997).

[71] A. V. Balatsky, I. Vekhter, and J.-X. Zhu, Rev. Mod. Phys. **78**, 373 (2006).

[72] W.-F. Tsai, Y.-Y. Zhang, C. Fang, and J. Hu, Phys. Rev. B **80**, 064513 (2009).

[73] M. Ruby, Y. Peng, F. von Oppen, B. W. Heinrich, and K. J. Franke, Phys. Rev. Lett. **117**, 186801 (2016).

[74] V. Kaladzhyan, S. Hoffman, and M. Trif, Phys. Rev. B **95**, 195403 (2017).

[75] S. Körber, B. Trauzettel, and O. Kashuba, Phys. Rev. B **97**, 184503 (2018).

[76] R. Žitko, J. S. Lim, R. López, and R. Aguado, Phys. Rev. B **91**, 045441 (2015).

[77] A. Jellinggaard, K. Grove-Rasmussen, M. H. Madsen, and J. Nygård, Phys. Rev. B **94**, 064520 (2016).

[78] S. Kawabata, Y. Tanaka, A. A. Golubov, A. S. Vasenko, and Y. Asano, J. Magn. Magn. Mater. **324**, 3467 (2012).

[79] J. D. Sau and E. Demler, Phys. Rev. B **88**, 205402 (2013).

[80] F. Pientka, Y. Peng, L. Glazman, and F. von Oppen, Phys. Scripta **2015**, 014008 (2015).

[81] N. Hatter, B. W. Heinrich, M. Ruby, J. I. Pascual, and K. J. Franke, Nat. Commun. **6**, 8988 (2015).

[82] A. Sakurai, Progr. Theor. Exp. Phys. **44**, 1472 (1970).

[83] B. M. Andersen, I. V. Bobkova, P. J. Hirschfeld, and Y. S. Barash, Phys. Rev. Lett. **96**, 117005 (2006).

[84] S. Kawabata, Y. Asano, Y. Tanaka, A. A. Golubov, and S. Kashiwaya, Phys. Rev. Lett. **104**, 117002 (2010).

[85] Y. A. Bychkov and E. I. Rashba, J. Phys. C **17**, 6039 (1984).

[86] P. G. De Gennes, *Superconductivity of Metals and Alloys* (Addison Wesley, Redwood City, 1989).

[87] M. J. M. de Jong and C. W. J. Beenakker, Phys. Rev. Lett. **74**, 1657 (1995).
[88] I. Žutić and O. T. Valls, Phys. Rev. B **60**, 6320 (1999).
[89] I. Žutić and O. T. Valls, Phys. Rev. B **61**, 1555 (2000).
[90] Y. Zhi-Hong, Y. Yong-Hong, and W. Jun, Chin. Phys. B **21**, 057402 (2012).
[91] See Supplemental Material at http://link.aps.org/supplemental/10.1103/PhysRevB.98.134511, including Refs. [9–11,15,28, 58–65,67,84,86,92,97–101], for more details.
[92] C. W. J. Beenakker, Phys. Rev. Lett. **67**, 3836 (1991).
[93] Since momentum is not a good quantum number, we rather use a general index **n** that labels perturbed eigenmodes above and below the S gap.
[94] I. O. Kulik, Zh. Eksp. Teor. Fiz. **57**, 1745 (1969) [J. Exp. Theor. Phys. **30**, 944 (1970)].
[95] J. Nitta, T. Akazaki, H. Takayanagi, and T. Enoki, Phys. Rev. Lett. **78**, 1335 (1997).
[96] T. Koga, J. Nitta, T. Akazaki, and H. Takayanagi, Phys. Rev. Lett. **89**, 046801 (2002).
[97] W. L. McMillan, Phys. Rev. **175**, 559 (1968).
[98] J. P. Carbotte, Rev. Mod. Phys. **62**, 1027 (1990).
[99] P. Fulde and R. A. Ferrell, Phys. Rev. **135**, A550 (1964).
[100] I. Larkin and Y. N. Ovchinnikov, Zh. Eksp. Teor. Fiz. **47**, 1136 (1964) [Sov. Phys. JETP **20**, 762 (1965)].
[101] A. Brinkman and A. A. Golubov, Phys. Rev. B **61**, 11297 (2000).